Photoassociation spectroscopy of ^{87}Rb$_2$ $(5s_{1/2}+5p_{1/2})0_u^+$ long-range molecular states: Coupling with the $(5s_{1/2}+5p_{3/2})0_u^+$ series analyzed using the Lu-Fano approach

H. Jelassi, B. Viaris de Lesegno, and L. Pruvost*

Laboratoire Aimé Cotton, CNRS II, Université Paris Sud, batiment 505, Campus d'Orsay, 91405 Orsay Cedex, France

We report on photoassociation of cold ^{87}Rb atoms providing the spectroscopy of $(5s_{1/2}+5p_{1/2})0_u^+$ long-range molecular states, in the energy range of $[-12.5, -0.7 \text{ cm}^{-1}]$ below the dissociation limit. A Lu-Fano approach coupled to the LeRoy-Bernstein formula is used to analyze the data. The Lu-Fano graph exhibits the coupling of the molecular series with the $(5s_{1/2}+5p_{3/2})0_u^+$ one, which is due to spin effects in the molecule. A two-channel model involving an improved LeRoy-Bernstein formula allows us to characterize the molecular series, to localize $(5s_{1/2}+5p_{3/2})0_u^+$ levels, to evaluate the coupling, and to predict the energy and width of the first predissociated level of $(5s_{1/2}+5p_{3/2})0_u^+$ series. An experimental spectrum confirms the prediction.

PACS number(s): 33.15.Ta, 32.80.Pj, 33.15.Pw, 33.20.Tp

I. INTRODUCTION

The photoassociation (PA) of cold atoms, which was proposed in 1987 [1] and demonstrated in 1993 [2], has become one of the more precise techniques for spectroscopy of long-range molecular states [3]. Especially for the alkali-metal dimers, this technique has been fruitful for the molecular states belonging to series that converge to the first $s+p$ dissociation limits, i.e., $s_{1/2}+p_{1/2}$ and $s_{1/2}+p_{3/2}$, if the spin-orbit interaction of the atom is taken into account. PA spectroscopy provides data concerning the energy levels and the photoassociation rate. Consequently these measurements can be connected to properties of the fundamental molecular potential. All these data are very important for studies of cold molecules, of atom-atom collisions, of atom-molecule collisions, etc. The energy positions of the bound states are essential data for the determination of the molecular parameters and therefore for the molecular curves.

The quantitative analysis of the energy positions of long-range molecular states are often done by fitting procedures using, for example, the LeRoy-Bernstein formula or the Rydberg-Klein-Rees method coupled to numerical computations. Such approaches lead to a correct determination of the asymptotic form of the potential, in particular a determination of the coefficients of the multipolar expansion. Furthermore, the use of the LeRoy-Bernstein formula [4] can be quantitatively completed by introducing the Lu-Fano graph method [5]. Such an approach has been applied to the long-range $(5s_{1/2}+5p_{1/2})0_g^-$ states of ^{87}Rb$_2$ [6]. In that case, which can be described by a one-channel model, an improved LeRoy-Bernstein formula [7,6] including an additional linear energy term is well adapted for a quantitative analysis. The origin of the additional term is in the short-range effects, namely, the repulsive barrier and the potential well.

In this paper, we present experimental results obtained for the long-range $(5s_{1/2}+5p_{1/2})0_u^+$ molecular states of ^{87}Rb$_2$ by using a trap loss PA spectroscopy technique. Then, we examine the data by using an approach involving both the LeRoy-Bernstein formula and the Lu-Fano graph. Due to spin-orbit

and spin-spin interactions the $(5s_{1/2}+5p_{1/2})0_u^+$ molecular curve is coupled to the $(5s_{1/2}+5p_{3/2})0_u^+$ one. The problem can thus be viewed as a two-channel problem. In a similar way to that used for Rydberg atom spectroscopy, we apply the Lu-Fano method to the molecular data. We show that the Lu-Fano graph exhibits the coupling effect. A two-series model including an improved LeRoy-Bernstein formula is then applied to characterize the series and to evaluate the coupling and the wave-function mixing. Furthermore, the location and width of the first predissociated level of the $(5s_{1/2}+5p_{3/2})0_u^+$ series are predicted. An experimental spectrum gives a confirmation of the predictions.

II. EXPERIMENT

The experiment is performed on ^{87}Rb atoms, trapped in a magneto-optical trap (MOT). The PA is realized with a tunable titanium-sapphire laser (Coherent MBR 110 system) red detuned from the D_1 line at 795 nm. The PA process is analyzed by using the trap loss spectroscopy technique [8]. It consists of recording the trap fluorescence (proportional to the atom number) while the PA laser is frequency scanned. If the laser wavelength is resonant with a molecular state, the PA creates long-range excited molecules. These excited molecules, having a very short lifetime, rapidly decay either to molecules in a vibrational state of the ground-state molecular curve or to fast free atoms. In both cases, the produced species cannot be trapped in the MOT and an atom loss is observed.

Details about the setup can be found in [6]. Details about the MOT realization are given in [9,10]. For this experiment the parameters are the following: a background Rb pressure in the 10^{-9} mbar range, a quadrupolar magnetic gradient of 14 G/cm, a few milliwatts per trapping laser beam (8 mm diameter), a trapping laser detuning of the $5s_{1/2}F=2 \rightarrow 5p_{3/2}F'=3$ rubidium line of -2Γ (Γ being the natural linewidth of $5p_{3/2}F'=3$ level, $\Gamma/2\pi=5.89$ MHz). Clouds of $\sim 10^7$ atoms with a ~ 0.5 mm radius and 30 μK temperature are obtained.

The PA spectrum is obtained by scanning the PA laser wavelength and by simultaneously recording the cloud fluo-

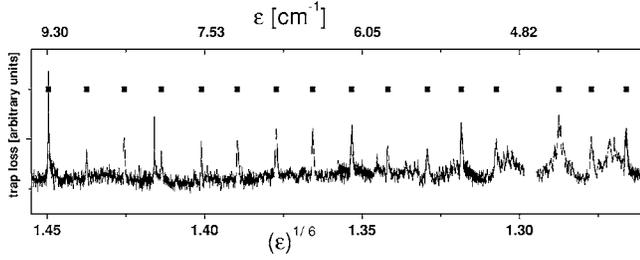*Email address: laurence.pruvost@lac.u-psud.fr

FIG. 1. Trap loss (shown as a positive signal) in the PA spectrum of ^{87}Rb near the dissociation limit, versus the energy, using a $\epsilon^{1/6}$ scale. Squares indicate the location of 0_u^+ resonances.

TABLE I. Long-range potential: the c_n parameters in the two first terms of the multipolar development in the nonrelativistic case; values of $R_{1/100}$ and $\epsilon_{1/100}$, obtained for the second term smaller than the first term by a 1/100 factor.

$V_1(R)$	Expression	Value
First term	$c_3 = \frac{4}{3}C_3$	11.932 a.u. [11]
Second term	$c_6 = \frac{2C_6^{\Pi}+C_6^{\Sigma}}{3} + \frac{4C_3^2}{27A}$	2.64×10^4 a.u. [12]
$R_{1/100}$		60.5 a.u.
$\epsilon_{1/100}$		12 cm^{-1}

rescence, which is proportional to the atom number in the trap. About 500 mW of laser light with a 1 mm diameter, slightly larger than the MOT size, is applied to the MOT. The wavelength measurement is done using a wavemeter (Burleigh WA 1100) with an accuracy of 500 MHz ($\sim$0.017 cm^{-1}). The fluorescence, collected onto a photodiode and amplified, is averaged and stored in a computer with a repetition rate of $\sim$4 Hz. Typically, the PA laser scans range 1 cm^{-1} during 600 s. Manual tunings are required to cover a wide range.

The molecular levels near the $5p_{1/2}$ limit have been explored. The PA spectrum (Fig. 1) exhibits vibrational progressions corresponding to the 1_g, 0_u^+, and 0_g^- molecular states. The 0_u^+ levels have been identified in the energy range -12.5 to -0.7 cm^{-1}, the energy being referenced relative to the molecular dissociation limit ^{87}Rb$(5s_{1/2})+^{87}$Rb$(5p_{1/2})$. The measured energy positions are reported in Table II below.

III. DESCRIPTION USING A LONG-RANGE POTENTIAL

A. Molecular potential

Because the spin-orbit interaction in the atom is larger than the binding energy of the long-range molecule, we describe the dimer on the basis of Hund's case (c). In this basis, for large values of the internuclear distance R, the molecular potentials can be expanded using a multipolar development. Considering only the two first terms of the development, the long-range potential curve $V_1(R)$ converging to the $(5s_{1/2}+5p_{1/2})$ dissociation limit is given by

$$V_1(R) = -c_3/R^3 - c_6/R^6 \tag{1}$$

where c_n ($n=3,6$) are coefficients related to atomic matrix elements as defined in [7]. Table I gives the expressions and values of the c_n coefficients in the nonrelativistic case. In the asymptotic range, as considered in this paper, the second term of $V_1(R)$ is negligible. Table I indicates also the values $R_{1/100}$ of the internuclear distance and the associated binding energy $\epsilon_{1/100}$ obtained for the second term smaller than the first term by a 1/100 factor.

A more elaborate description of the molecule leads one to take into account other interactions. First, one has to add the spin-orbit interaction in the molecule, the spin-spin interaction, and weaker terms such as hyperfine effects. The spin-orbit interaction in the molecule includes the atomic fine

structure which is already considered in Hund's case (c), and the interaction between the spin and the "other" orbit around the second atom of the dimer [13]. In alkali-metal dimers, this term can be of the same order of magnitude as the spin-spin interaction [14,15]. These two terms, which we denote "spin effects in the molecule," introduce a coupling between $V_1(R)$ and the potential curve $V_2(R)$ converging to the higher-energy dissociation limit $(5s_{1/2}+5p_{3/2})$. According to other studies [14,15], the coupling is large for short internuclear distances. For a long-range molecule, the coupling is more weakly energy dependent. This remark will allow us to consider it as a constant over the studied energy range.

B. The LeRoy-Bernstein formula

In the case of an asymptotic attractive molecular potential written as $V(R)=D-c_n/R^n$, with $n \geq 2$, with R the internuclear distance, D the dissociation limit, and c_n the multipole expansion coefficient, it has been demonstrated [4] that the binding energy ϵ_v of a vibrational level labeled v is given by

$$\epsilon_v = \epsilon_n (v_D - v)^{2n/(n-2)} \tag{2}$$

with v_D a noninteger number, and ϵ_n an energy constant related to c_n and the reduced mass μ. The expression for ϵ_n is $\epsilon_n = H_n^{2n/(n-2)}$ where the usual H_n coefficient is given by $H_n^{-1} = \frac{\sqrt{2\mu}}{\sqrt{\pi}} \frac{c_n^{1/n}}{\hbar(n-2)} \frac{\Gamma(1/2+1/n)}{\Gamma(1+1/n)}$, Γ being the Gamma function.

In the usual analysis, the LeRoy-Bernstein formula is used to fit the energy positions. Such a procedure provides values for v_D and ϵ_n. If the dissociation limit is not perfectly known, a shift of the energy is introduced as an additional fitting parameter. Such an analysis is particularly adapted for long-range states and for a one-channel problem.

Nevertheless, even for large R values, it is rare that one molecular curve can be treated completely independently of the neighboring potentials, belonging to the molecular diagram. In the studied example, due to spin effects in the molecule, $V_1(R)$ is coupled to the potential of the $(ns_{1/2}+np_{3/2})$ series. Therefore, due to the couplings, the ϵ_v values given by the LeRoy-Bernstein formula are slightly changed. A precise analysis of these changes requires one to obtain information about the coupling and about the states belonging to the neighboring potential. Often, it is quite difficult to evaluate the coupling, because the energy measured in an experiment via the binding energy is dominated by the long-range potential value.
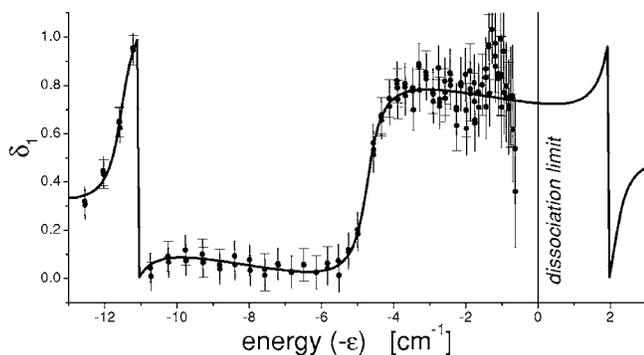
FIG. 2. Energy Lu-Fano plot for the ^{87}Rb$_2$ $(5s_{1/2}+5p_{1/2})0_u^+$ levels (points) and the fitting curve.

C. Lu-Fano graph

The Lu-Fano approach has been fruitfully applied to the Rydberg atom spectroscopy (for a review see [16,17]). It leads to a simple and precise characterization of each Rydberg series. For a single-channel model (one uncoupled potential), the series can be fully characterized by only one parameter, the quantum defect μ, which is nearly energy independent. Then the binding energy of the level labeled n varies as $1/(n-\mu)^2$. For two coupled channels, the Lu-Fano plot leads to a full characterization of the system with three parameters: the quantum defects of each nonperturbed channel μ_1 and μ_2 and a coupling parameter K. For Rydberg atoms and in many models, the three parameters μ_1, μ_2, and K are nearly independent of the energy.

The analysis of long-range molecular states can be done by this method. The energy Lu-Fano plot is created from the experimental data: for each level, the measured binding energy ϵ is expressed as an effective vibrational quantum number v^* via an assumed law; then the quantum defect defined by $\delta=v^*-\text{int}[v^*]$ is plotted versus the energy. In our case, the law is the LeRoy-Bernstein formula with $n=3$, i.e., $\epsilon=\epsilon_3 v^{*6}$. If the energy law is satisfied, the quantum defect δ is constant and the energy Lu-Fano plot is a horizontal line. This constant is usually denoted μ. The LeRoy-Bernstein formula gives $\mu=v_D-\text{int}[v_D]$. If the energy Lu-Fano plot shows deviations from a horizontal line, they can be mainly attributed to an imperfect LeRoy-Bernstein formula [6] or/ and to couplings with other molecular potentials.

In the considered energy range, the $(5s_{1/2}+5p_{1/2})0_u^+$ molecular potential is described by the asymptotic law which permits the use of the LeRoy-Bernstein formula. The energy law is illustrated in Fig. 1 with a nearly equidistant spacing of the levels on an energy scale proportional to $\epsilon^{1/6}$. The energy Lu-Fano plot deduced from the data is shown in Fig. 2.

The Lu-Fano plot exhibits two sharp variations at $\epsilon\sim 11.5$ and $\epsilon\sim 4.5$ cm^{-1}. They are the signature of perturbations of the energy positions of the $(5s_{1/2}+5p_{1/2})0_u^+$ levels by two levels belonging to the $(5s_{1/2}+5p_{3/2})0_u^+$ series. Each step magnitude is about 0.8 compared to the value of 1 observed in the usual Lu-Fano plot.

IV. A TWO-CHANNEL MODEL

To evaluate the coupling between the two molecular curves V_1 and V_2, we propose a two-channel model in an approach similar to that used in Rydberg series studies. The simplest theoretical framework, assuming two infinite series having equidistant energy levels coupled via an off-diagonal constant coupling V, was treated by Demkov and Ostrovsky [18]. The diagonalization of such a system leads to the equation $\tan[\pi(\delta_1-\mu_1)]\times\tan[\pi(\delta_2-\mu_2)]=\pi^2 K^2$, where δ_i $(i=1,2)$ are the quantum defects defined relative to the energy equation $\epsilon=(n_i+\delta_i)\hbar\omega_i$, μ_i are the quantum defects associated with the nonperturbed series, and K is the coupling parameter defined by $K=V/(\hbar\sqrt{\omega_1\omega_2})$. In the case of coupled Rydberg series [16,17] with the use of the Rydberg equation $\epsilon=1/(n_i-\mu_i)^2$, one obtains the same equation. This equation was obtained for two series composed of an infinity of levels and described by the same energy equation. In the case of two coupled molecular curves, the same equation has been applied to present and analyze results of molecular numerical calculations [19–21].

Nevertheless, in many cases, the energy equation (analytic in our example, but it is not necessary for a general case) cannot be applied to $V_2(R)$ because the energy difference between the dissociation limits is large and the asymptotic form is not correct for $V_2(R)$. Furthermore, the number of molecular levels is finite. Thus, considering remarks made in Sec. II of [18], we propose an adapted form of the previous equation, applicable in a small energy interval:

$$\tan[\pi(\delta_1-\mu_1)]\times\tan\left[\pi\left(\frac{\epsilon-\epsilon_2}{\Delta_2}\right)\right]=\pi^2 K^2. \qquad (3)$$

μ_1 is the quantum defect that characterizes the nonperturbed series associated with V_1, ϵ_2 is the location of the perturbing level belonging to V_2, Δ_2 is the energy spacing between two successive perturbing levels, and K is the coupling parameter due to spin effects in the molecule.

Such a formula with μ_1 assumed to be a constant gives quantum defect steps of one unit and cannot describe the quantum defect of ~ 0.8 observed in Fig. 2. According to previous observations [6] and models [7,6], which take into account the short-range molecular curve (repulsive barrier and potential well), for weakly bound levels it has been shown that the LeRoy-Bernstein formula can be improved, leading to a linear variation of μ_1 versus the energy as

$$\mu_1=\mu_{1\infty}-\gamma\epsilon, \qquad (4)$$

where $\mu_{1\infty}$ is the quantum defect at the dissociation limit and γ is a global parameter for short-range potential effects.

The energy Lu-Fano plot of Fig. 2 has been fitted using both Eqs. (3) and (4), providing the following values: $\mu_{1\infty}=0.6932\pm0.0166$, $\gamma=-0.0448\pm0.0031(\text{cm}^{-1})^{-1}$, $\epsilon_2=4.724\pm0.066$ cm^{-1}, $\Delta_2=6.803\pm0.084$ cm^{-1}, and $K=0.1221\pm0.0086$.

A. Characterization of the $(5s_{1/2}+5p_{1/2})$ series

The values of $\mu_{1\infty}$ and γ give a characterization of the nonperturbed molecular series V_1 with only two parameters. As proposed in Ref. [6], simple analytical models allow one

to link the γ value to the position of the repulsive barrier of the molecular potential. In the model assuming only a c_3/R^3 long-range behavior limited by a vertical barrier at $R=R'_c$, one deduces $R'_c=17.82$ a.u. Considering, moreover, the value of $\mu_{1\infty}$, a more elaborate model with a constant potential between $R=R'_c$ and $R=R_c$ leads to $R'_c=17.9$ a.u. and $R_c=19.3$ a.u. Such models, not valid for molecular states with large binding energy, are pertinent for a determination of the long-range molecular wave functions. Such calculations are useful for numerical predictions of processes including excitation of long-range molecules, for example, for cold molecule formation.

B. States of the $(5s_{1/2}+5p_{3/2})$ series

The values of ϵ_2 and Δ_2 give the energy positions of two levels of the $(5s_{1/2}+5p_{3/2})0_u^+$ series located, respectively, at $\epsilon_2+\Delta_2=11.527$ cm^{-1} and $\epsilon_2=4.724$ cm^{-1} below the $(5s_{1/2}+5p_{1/2})$ dissociation limit [or 249.125 and 242.322 cm^{-1} below the $(5s_{1/2}+5p_{3/2})$ dissociation limit]. In this region, a multipolar expansion of the potential $V_2(R)=D_2-14.915/R^3+5149/R^6$ (in atomic units) allows one to check that the LeRoy-Bernstein formula cannot be applicable for V_2, and gives the values of the outer classical turning points corresponding to these energies: $R_M=23.38$ a.u. and $R_M=23.61$ a.u. These values are small compared to the turning points of V_1, respectively, 61.1 and 82.3 a.u., and indicate excitation at intermediate internuclear distances.

C. Coupling and predissociated states

The coupling parameter is related to the coupling V by $V=K\sqrt{\Delta_1\Delta_2}$ where Δ_i ($i=1,2$) are the energy spacings between two successive levels. Using $\Delta_1=6H_3\epsilon^{5/6}$ we thus deduce $V=0.16$ cm^{-1} at the second step (4.724 cm^{-1} below the dissociation limit). Considering the nonperturbed positions of the series 1, which are given by $\epsilon=(H_3v_1^*)^6$ and $v_1^*-\mathrm{int}(v_1^*)=\mu_1=\mu_{1\infty}-\gamma\epsilon$, we also deduce the energy difference Δ between the perturbing level and the closest level of the series 1: $\Delta=0.079$ cm^{-1}. We conclude a ratio $\Delta/V=0.49$ which indicates a large coupling in this region. The coupling can also be expressed by the angle θ, defined by $\tan(2\theta)=V/\Delta$ and related to the wave-function mixing. The values give $\theta=31.8°$, a 45° angle corresponding to the maximum expected coupling. The value of 31.8° indicates an efficient mixing between $(5s_{1/2}+5p_{1/2})$ states and the $(5s_{1/2}+5p_{3/2})$ state. That result is of great interest in the context of cold molecule formation [22].

Because we have evaluated the coupling in the vicinity of the dissociation limit and assuming that the energy spacing is nearly constant, we extrapolate the Lu-Fano plot (Fig. 2) and predict the position of the first predissociated level of the $(5s_{1/2}+5p_{3/2})0_u^+$ series. It is located at ~2.1 cm^{-1} above the $(5s_{1/2}+5p_{1/2})$ dissociation limit. Applying the Fermi golden rule, its width is given by $\Gamma=(2\pi/\hbar)(V^2/\Delta_1)=(2\pi/\hbar)K^2\Delta_2$, and is estimated to be about 4 cm^{-1}. These values are in good agreement with [23] and with previous calculations [19].
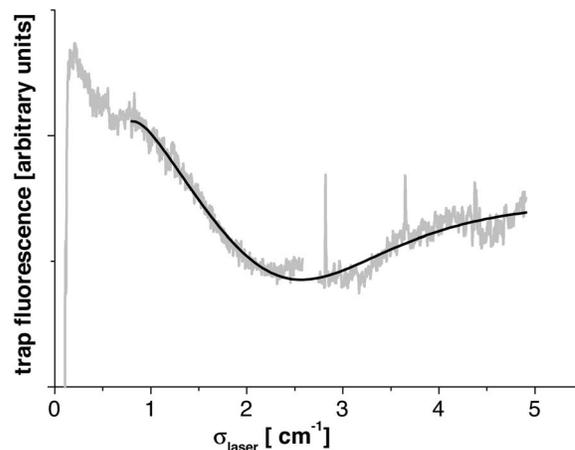

FIG. 3. Trap fluorescence signal (gray line) recorded above the $(5s_{1/2}+5p_{1/2})$ dissociation limit: the broad negative resonance located at ~2.5 cm^{-1} corresponds to a predissociated level of the $(5s_{1/2}+5p_{3/2})0_u^+$ series; the three narrow peaks, corresponding to PA laser zero intensity, are used to calibrate the signal; the nonhorizontal fluorescence baseline is due to the light shift induced by the PA laser on the atoms, except close to the atomic resonance (typically less than 0.7 cm^{-1}), where the PA laser strongly modifies the trap behavior. The fitting function (black line) includes the PA light shift and the predissociation profile.

Furthermore, they are confirmed by the spectrum presented in Fig. 3 which is a record of the trap fluorescence a few wave numbers above the $(5s_{1/2}+5p_{1/2})$ dissociation limit. The predissociation resonance is the broad negative shape centered at 2.5 cm^{-1}. This resonance appears on a non-horizontal baseline. Taking into account the light shift induced by the PA laser on the atoms, the fluorescence baseline is expected to vary as the inverse of the wave number, except close to the atomic resonance (typically less than 0.7 cm^{-1}), where the PA laser strongly modifies the trap behavior by pushing the atoms and unbalancing the trapping forces. A fit of the trap fluorescence, including light-shift effect and a Lorentzian shape for the predissociation resonance, gives a location at 2.32 ± 0.01 cm^{-1} and a width of 3.14 ± 0.04 cm^{-1}, the values being in good agreement with the predicted ones.

V. CONCLUSION

In summary, we have presented an experimental study of $(5s_{1/2}+5p_{1/2})0_u^+$ levels in the asymptotic range, allowing the application of the LeRoy-Bernstein formula. Coupling this formula to the Lu-Fano method, we deduce a Lu-Fano graph which exhibits the coupling to the $(5s_{1/2}+5p_{3/2})$ series. We propose a two-channel model with a quantum defect linearly dependent on the energy to extract quantitative parameters such as the quantum defects and the coupling parameter. Furthermore, it leads to a prediction about previously unobserved molecular levels, for example, predissociated levels with very short lifetimes. The method, successfully applied here to the rubidium molecule, would be fruitful for other molecular species. Only the long-range potential form is required to analyze the data and deduce other molecular constants.

TABLE II. ^{87}Rb $(5s_{1/2}+5p_{1/2})0_u^+$ levels: experimental binding energy measured relative to the atomic transition ^{87}Rb$(5s_{1/2}, F=2) \rightarrow {}^{87}Rb(5p_{1/2})$ at 12 578.780 cm^{-1}. The first column gives int[v^*].

int[v^*]	ϵ[cm^{-1}]	int [v^*]	ϵ[cm^{-1}]
127	12.552; 12.545; 12.542	100	3.101; 3.098; 3.096
126	12.035; 12.036; 12.040; 12.043; 12.036	99	2.907; 2.907; 2.905; 2.900
125	11.595; 11.594; 11.596; 11.593; 11.581	98	2.753; 2.731; 2.729; 2.726
124	10.734; 10.716; 10.716	97	2.581; 2.574; 2.574; 2.570
123	10.249; 10.248; 10.237	96	2.432; 2.431; 2.427; 2.424
122	9.772; 9.753; 9.751	95	2.264; 2.264; 2.263; 2.254
121	9.294; 9.279; 9.278	94	2.140; 2.139; 2.139; 2.139
120	8.824; 8.823; 8.816	93	2.013; 1.994; 1.994; 1.984
119	8.407; 8.391	92	1.889; 1.880; 1.878
118	7.985; 7.968	91	1.756; 1.765; 1.747; 1.745
117	7.573; 7.564	90	1.648; 1.648; 1.641
116	7.202; 7.200	89	1.545; 1.545
115	6.826; 6.824	88	1.451; 1.448; 1.436
114	6.487; 6.487	87	1.365; 1.364; 1.347
113	6.143; 6.143	87	1.280; 1.280
112	5.836; 5.829	85	1.190; 1.185; 1.182
111	5.533; 5.515	84	1.099; 1.098; 1.098
110	5.254; 5.251	83	1.034; 1.024; 1.023; 1.023; 1.014
109	4.997; 4.992	82	0.959; 0.947
107	4.563; 4.551; 4.556	81	0.882; 0.879
106	4.342; 4.341; 4.337; 4.340	80	0.815; 0.814
105	4.120; 4.120; 4.120; 4.112	79	0.758; 0.758
104	3.908; 3.905; 3.902; 3.901; 3.891; 3.890	78	0.703; 0.696
103	3.687; 3.684; 3.676	77	0.640; 0.631
102	3.475; 3.475; 3.473; 3.457		
101	3.296; 3.294; 3.276		

ACKNOWLEDGMENTS

APPENDIX

We give in Table II the measured binding energy ϵ of the ^{87}Rb$_2$ $(5s_{1/2}+5p_{1/2})0_u^+$ levels. The first column gives int[v^*] where $\epsilon = \epsilon_3 v^{*6}$. The 0_u^+ levels are obtained via the transition ^{87}Rb $(5s_{1/2}, F=2) + {}^{87}$Rb $(5s_{1/2}, F=2) + h\nu_{PA} \rightarrow {}^{87}Rb_2(5s_{1/2}+5p_{1/2})0_u^+$ where ν_{PA} indicates the frequency of the PA laser light. The wave-number measurement is given relative to the atomic transition ^{87}Rb $(5s_{1/2}, F=2) \rightarrow {}^{87}$Rb $(5p_{1/2})$ at 12 578.780 cm^{-1}.

[1] H. R. Thorsheim, J. Weiner, and P. S. Julienne, Phys. Rev. Lett. **58**, 2420 (1987).

[2] P. D. Lett, K. Helmerson, W. D. Phillips, L. P. Ratliff, S. L. Rolston, and M. E. Wagshul, Phys. Rev. Lett. **71**, 2200 (1993).

[3] W. C. Stwalley and H. Wang, J. Mol. Spectrosc. **195**, 194 (1999).

[4] R. J. LeRoy and R. B. Bernstein, J. Chem. Phys. **52**, 3869 (1970).

[5] K. T. Lu and U. Fano, Phys. Rev. A **2**, 81 (1970).

[6] H. Jelassi, B. Viaris De Lesegno, and L. Pruvost, Phys. Rev. A **73**, 032501 (2006).

[7] D. Comparat, J. Chem. Phys. **120**, 1318 (2004).

[8] H. Wang, P. L. Gould, and W. C. Stwalley, Phys. Rev. A **53**, R1216 (1996).

[9] L. Pruvost, D. Marescaux, O. Houde, and H. T. Duong, Opt. Commun. **166**, 199 (1999).

[10] D. Kadio, O. Houde, and L. Pruvost, Europhys. Lett. **54**, 417 (2001).

[11] We take $C_3 = 8.949(10)$ a.u. as explained in [6].

[12] We take $A = 158.398\,936\,62$ cm$^{-1} \equiv 7.217\,186\,589\,2 \times 10^{-4}$ a.u., $C_6^{\Pi} = 8.05 \times 10^3$ a.u., $C_6^{\Sigma} = 12.91 \times 10^3$ a.u., thus $(4/27)C_3^2/A = 1.6439 \times 10^4$ a.u.; $(2C_6^{\Pi} + C_6^{\Sigma})/3 = 0.997 \times 10^4$ [6].

[13] B. H. Brandsen and C. J. Joachain, *Physics of Atoms and Molecules* (Longmans, New York, 1983).

[14] F. H. Mies, C. J. Williams, P. S. Julienne, and M. Krauss, J. Res. Natl. Inst. Stand. Technol. **101**, 521 (1996).

[15] P. J. Leo, E. Tiesinga, P. S. Julienne, D. K. Walter, S. Kadlecek, and T. G. Walker, Phys. Rev. Lett. **81**, 1389 (1998).

[16] M. J. Seaton, Rep. Prog. Phys. **46**, 167 (1983).

[17] M. Aymar, C. H. Greene, and E. Luc-Koenig, Rev. Mod. Phys. **68**, 1015 (1996).

[18] Y. N. Demkov and V. N. Ostrovsky, J. Phys. B **28**, 403 (1995).

[19] V. Kokoouline, O. Dulieu, and F. Masnou-Seeuws, Phys. Rev. A **62**, 022504 (2000).

[20] V. N. Ostrovsky, V. Kokoouline, E. Luc-Koenig, and F. Masnou-Seeuws, J. Phys. B **34**, L27 (2001).

[21] V. Kokoouline, C. Drag, P. Pillet, and F. Masnou-Seeuws, Phys. Rev. A **65**, 062710 (2002).

[22] C. M. Dion, C. Drag, O. Dulieu, B. Laburthe Tolra, F. Masnou-Seeuws, and P. Pillet, Phys. Rev. Lett. **86**, 2253 (2001).

[23] R. A. Cline, J. D. Miller, and D. J. Heinzen, Phys. Rev. Lett. **73**, 632 (1994).